High-content analysis of larval phenotypes for the screening of xenobiotic toxicity using Phallusia mammillata embryos

Ievgeniia Gazo, Isa Gomes, Thierry Savy, Nadine Peyriéras, Lydia Besnardeau, Celine Hebras, Sameh Benaicha, Manon Brunet, Olena Shaliutina, Alex Mcdougall, et al.

High-content analysis of larval phenotypes for the screening of xenobiotic toxicity using *Phallusia mammillata* embryos

Ievgeniia Gazo[1,2*], Isa D. L. Gomes[1], Thierry Savy[3], Nadine Peyrieras[3], Lydia Besnardeau[1], Celine Hebras[1], Sameh Benaicha[1], Manon Brunet[1], Olena Shaliutina[2], Alex McDougall[1] and Rémi Dumollard[1]

[1] Sorbonne Universités, UPMC Univ Paris 06, CNRS, Laboratoire de Biologie du Développement de Villefranche-sur-mer (LBDV), Observatoire Océanologique, 06230 Villefranche sur-mer, France

[2] University of South Bohemia in Ceske Budejovice, Faculty of Fisheries and Protection of Waters, South Bohemian Research Center of Aquaculture and Biodiversity of Hydrocenoses, Research Institute of Fish Culture and Hydrobiology, Zátiší 728/II, 389 25, Vodňany, Czech Republic

[3] BioEmergences Laboratory, CNRS USR 3695, 91190 Gif-sur-Yvette, France

* Corresponding author: I. Gazo; Zátiší 728/II, 389 25, Vodňany, Czech Republic; gazo@frov.jcu.cz

Abstract

In recent years, pollution of surface waters with xenobiotic compounds became an issue of concern in society and has been the object of numerous studies. Most of these xenobiotic compounds are man-made molecules and some of them are qualified as endocrine disrupting chemicals (EDCs) when they interfere with hormones actions. Several studies have investigated the teratogenic impacts of EDCs in vertebrates (including marine vertebrates). However, the impact of such EDCs on marine invertebrates is much debated and still largely obscure. In addition, DNA-altering genotoxicants can induce embryonic malformations. The goal of this study is to develop a reliable and effective test for assessing toxicity of chemicals using embryos of the ascidian (*Phallusia mammillata*) in order to find phenotypic signatures associated with xenobiotics. We evaluated embryonic malformations with high-content analysis of larval phenotypes by scoring several quantitative and qualitative morphometric endpoints on a single image of *Phallusia* tadpole larvae with semi-automated image analysis. Using this approach we screened different classes of toxicants including genotoxicants, known or suspected EDCs and nuclear receptors (NRs) ligands.

The screen presented here reveals a specific phenotypic signature for ligands of retinoic acid receptor/retinoid X receptor. Analysis of larval morphology combined with DNA staining revealed that embryos with DNA aberrations displayed severe malformations affecting multiple aspects of embryonic development. In contrast EDCs exposure induced no or little DNA aberrations and affected mainly neural development. Therefore the ascidian embryo/larval assay presented here can allow to distinguish the type of teratogenicity induced by different classes of toxicants.

Keywords: ascidian; embryo; toxicity; morphological analysis; endocrine disrupting chemical (EDC); genotoxicity

1. INTRODUCTION

Anthropogenic activities have a large impact on aquatic ecosystems from the discharge of chemical substances, many of which are supposed to be present in trace amounts (i.e. heavy metals) or even absent in natural conditions (i.e. pharmaceuticals, pesticides) (Mnif et al., 2011; Desbiolles et al., 2018). Endocrine disrupting chemicals (EDCs) are xenobiotic substances that can interfere with the endocrine system through two main pathways: the genomic pathway, via binding to nuclear receptors (NRs); or the non-genomic pathway, via binding to cell membrane receptors or affecting hormone metabolism. Thus endocrine disruption can be induced by xenobiotics that bind nuclear receptors such as AR, ER, TR, PPAR, RXR, PXR, CAR or ERR (termed NR-binding EDCs) (Mnif et al., 2011). Upon NR binding, EDCs can either activate a receptor (agonist action) or block it for normal hormone (antagonistic action).

Many phenotypes of EDCs exposure have been described in invertebrate species (Urushitani et al., 2018; Castro et al., 2007; le Maire et al., 2009; Nishikawa et al., 2004; Matsushima et al., 2013), but the mode-of-action of these EDCs remains mainly unclear. One approach to predict whether a xenobiotic might target a NR is to compare its phenotype against the phenotypes produced by a specific NR agonist/antagonist (Tohmé et al., 2014, Gomes et al., 2019b). If a phenotypic signature can be associated with a specific NR agonist/antagonist, then it can be potentially used as a biomarker of NR-signaling disruption.

In the past years, ascidian species have been used as toxicological models (reviewed in Dumollard et al., 2017; Zega et al., 2009; Gallo and Tosti, 2015; Battistoni et al., 2018). Ascidians are marine filter-feeding chordates belonging to the Subphylum Urochordata, recognized as the sister group of vertebrates (Delsuc et al., 2006). Their zygotes divide 13 to 15 times in 18 hours to give rise to

63 a transparent vertebrate-like tadpole larvae (Yamada and Nishida, 2014). The ascidian larva
64 possesses both central and peripheral nervous system (CNS and PNS) (reviewed in Hudson, 2016;
65 Dumollard et al., 2017; Gomes et al., 2019a). The CNS of ascidian larvae is composed of a sensory
66 vesicle and a motor ganglion homologous, respectively, to the vertebrate diencephalon and
67 hindbrain (Holland and Holland, 1999). The sensory vesicle within the CNS contains two easily
68 identifiable dark pigmented sensory organs (PSO), the otolith (Ot) and the ocellus (Oc). The PNS
69 consists of the papillary neurons in palps, the epidermal sensory neurons, and the bipolar tail
70 neurons (Hudson, 2016). A prominent feature of ascidian larva are the adhesive organs, or palps,
71 which are part of the PNS (Takamura, 1998). Hence, a number of morphological features can be
72 assessed in the transparent ascidian larva to discriminate between non specific teratogenicity (i.e.
73 problems in general morphogenesis of the larva) and specific neurodevelopmental toxicity (i.e.
74 problems in the development of PNS and CNS structures). Ascidian neurodevelopment might be
75 especially sensitive to NR-targeting EDCs as several NRs are expressed in neurogenic domains of
76 the ascidian embryo (reviewed in Gomes et al., 2019a).

77 High-content analysis is a technique that involves scoring of multiple endpoints on a single image
78 which can be achieved by automated or semi-automated image analysis and is now commonly
79 applied to drug discovery screening using biological systems (Esner et al., 2018). The aim of this
80 study was to analyse the teratogenic effects of different classes of compounds (EDCs, NR ligands,
81 genotoxic and cytotoxic compounds) by quantifying larval malformations of the ascidian *Phallusia*
82 *mammillata*. We have hypothesized that by performing high-content analysis of morphological
83 malformations in *Phallusia* tadpole larvae, we will determine phenotypic signatures of different
84 types of compounds, such as a toxicant (sodium azide), genotoxicants (TBT, etoposide, mitomycin
85 C), known/susptected EDCs (lindane, atrazine, chlordane, chlorpyrifos, BPA, estradiol benzoate)

and nuclear receptors (NRs) ligands. Etoposide, TBT, and mitomycin were used as reference genotoxic compounds (Kirkland et al., 2016). The pesticides analyzed in the current study (lindane, atrazine, chlordane, chlorpyrifos), as well as BPA, are often referred to as EDCs (Mnif et al., 2011); however, their mechanism of action in marine invertebrates is unknown. Our previous work showed that several NRs (RAR, PXR/VDRα, PPAR, ROR, and ERR) are expressed in neurogenic regions of *Phallusia mammillata* embryos (Gomes et al., 2019a, Gomes et al., 2019b). We analyzed known agonists/antagonists of these NRs, such as UVI3003 (RXR antagonist), all-trans retinoic acid (RAR agonist), rifampicin and SR12813 (PXR agonists), SR1078 (ROR agonist), BADGE (PPAR agonist), diethylstilbestrol, and 4-hydrotamoxifen (ERR antagonists).

To complement our morphometric analysis of embryonic development we also performed a genotoxicity assay. Genotoxicity is the loss of DNA structural or functional integrity. There are several protocols for analysing DNA damage induced by genotoxic compounds (OECD test N. 487; OECD test N. 473; OECD test N. 489) and some of them have been successfully applied to marine invertebrates (Dixon et al., 2002; Saotome et al., 1999;). However, it is not clear which phenotypic signature is associated with DNA damage and genotoxicity in the embryo. The ascidian embryo is an interesting model for scoring genotoxicity, since the spindle assembly checkpoint is not active at early stages of development (Chenevert et al., 2020). Thus, even upon DNA damage the embryo will continue dividing without pausing to repair DNA damage, resulting in overt DNA aberrations such as micronuclei, multinucleated cells or DNA bridges.

We describe here methods for ascidian embryonic cultures and provide different morphological endpoints of the ascidan larva that can be scored to discriminate larval phenotypes. Such high content analysis of ascidian larval phenotypes can be coupled with DNA staining to correlate embryonic phenotypes with the level of genotoxicity. We show a first screen of 19 molecules using

these protocols and found that genotoxicants affect all morphological endpoints whereas EDCs and NR ligands affect mostly neural endpoints.

2. Materials & Methods

2.1. Animals

Phallusia mammillata were collected at Sète (Etang de Tau, Mediterranean coast, France) and kept in the aquaria of the "Centre de Ressources Biologiques" (CRB) of the Institut de la Mer à Villefranche (IMEV) which is an EMBRC-France certified service (see https://www.embrc-france.fr/fr/nos-services/fourniture-de-ressources-biologiques/organismes-modeles/ascidie-phallusia-mammillata). Animals were maintained in the aquaria on open system with running seawater (pH 8.2 ± 0.05, salinity 40 ± 0.5 ppt) at 16°C for at least two weeks before use. Animals were fed 3 to 5 times per week with commercial microalgae concentrates (2-3 mL per aquarium of 60 L), Shellfish diet 1800® and Isochrysis 1800® (Instant Algae®, Reed Mariculture Inc., Campbell, CA, USA, 95008) purchased from a french distributor. Ascidian eggs were collected by oviduct dissection. In order to ensure proper penetration of the studied compounds into eggs, they were dechorionated with 0.1% Trypsin (Sigma-Aldrich, T9201) in filtered sea water (FSW) for 60 min at 20°C, then transferred to fresh sea water and stored at 18°C until required. Sperm was collected by syringe aspiration from a sperm duct and was activated with high pH 9.2 sea water for 10–20 min, then used to fertilize dechorionated eggs (Gomes et al., 2019b; see full protocols on http://lbdv.obs-vlfr.fr/en/research/research_groups/ascidian-biocell-group/projets/fertilization-and-meiosis/protocols.html). The embryos were reared in dark conditions to avoid photodegradation of chemicals.

2.2. Tested Chemicals

Sodium azide (CAS Number: 26628-22-8; purity: ≥ 99%), tributyltin (CAS Number 1461-22-9; ≥ 96%), etoposide (CAS Number 33419-42-0; reference standard), atrazine (CAS Number 1912-24-

9; analytical standard), lindane (CAS Number 58-89-9; analytical standard), chlordane (CAS Number 5103-71-9; analytical standard), chlorpyrifos (CAS Number 2921-88-2; analytical standard), SR12813 (CAS Number 126411-39-0; ≥ 98%), diethylstilbestrol (CAS Number 56-53-1; ≥ 99%), 4-hydroxytamoxifen (CAS Number 68392-35-8; analytical standard), rifampicin (CAS Number 13292-46-1; ≥97% (HPLC)), mitomycin C (CAS Number 50-07-7; reference standard), bisphenol A (CAS Number 80-05-7; ≥ 99%), estradiol benzoate (CAS Number 50-50-0; ≥97% (HPLC)), ATRA (CAS Number 302-79-4; ≥ 98%), BMS493 (CAS Number 215030-90-3; ≥ 98%), and UVI3003 (CAS Number 847239-17-2; ≥ 98%) were purchased from the Sigma-Aldrich Co. (St Louis, MO, USA). BADGE (CAS Number 1675-54-3; ≥ 95%) and SR1078 (CAS Number 1246525-60-9; ≥98% (HPLC)) were purchased from Tocris Bioscience (Bristol, UK). Table 1 shows tested compounds and concentrations used in the current study. We have performed toxicity testing to determine the dose that will produce serious toxicological effects, therefore the concentrations used in the current study were mostly higher than environmentally relevant.

2.3. Experimental design

All compounds were resuspended in DMSO for a stock concentration. Immediately before the treatment, stock solutions were diluted with DMSO to a 10 000x working concentration. Finally, prediluted stocks were added to the embryo culture medium (FSW, 5 mM TAPS, 0.5 mM EDTA, pH 8, salinity 40 ± 0.5 ppt) at 1:10 000 ratio giving the required concentration of a compound in the medium and 0.01% DMSO (v/v). The same amount of DMSO (0.01% in embryo culture medium) was used as a vehicle control. All solutions were controlled to be at pH 8 and prechilled to 18°C prior to embryo exposure. Concentrations of compounds were selected based on preliminary experiments. We have chosen the concentrations which induced malformations, but

were not lethal (i.e. which did not induce 100% undevelopped embryos) or the highest soluble concentration.

Dechorionated eggs (approximately 1000 eggs) were mixed with activated sperm (10^6/ml diluted in FSW) in the embryo culture medium for fertilization (Sardet et al., 2011; Gomes et al., 2019b). After fertilization, embryos were washed twice with FSW to remove excess of sperm and to avoid polyspermy. Washed embryos at 1-cell stage were then transferred to 12-well plates, each well is coated with GF (gelatin/formaldehyde, see Sardet et al., 2011), at a concentration of 100 embryos/well. Each well contained either vehicle control or a tested concentration of compound in a total of 3 mL of FSW. Plates with embryos were kept in dark humid chambers to avoid photodegradation of xenobiotics at 18°C. Embryos were left to develop to gastrula or neurula stage (7 – 9 hpf at 18°C) and ~30 embryos were collected for genotoxicity analysis (Supplementary Fig. 1). The rest of embryos was left to develop to swimming larval stage (stage 26, 22 hpf at 18°C; see Gomes et al., 2019b). Embryos were exposed to tested compounds from 1-cell stage till fixation.

When embryos in the control reached swimming larval stage, all cultures were fixed with 0.4% formaldehyde to stop motility. Fixed embryos were transferred to a chamber slide and imaged with a Zeiss Axiovert200 inverted microscope at 10X magnification. For each culture, a minimum of 30 embryos were analyzed per treatment (N = 30 technical replicates). Each experimental condition was repeated at least 3 times (n = 3 biological replicates).

2.4. Morphological analysis of phenotypes

Analysis of the phenotypes at larval stage was performed with Toxicosis, a software developed in our laboratory with a proprietary code and filed by the CNRS at the APP (Agency for the

Protection of Programs) on July 13th 2018 under the reference IDDN.FR.001.330013.000.S.P.2018.000.10000. The analyzed endpoints are summarized in Supplementary Figure 2 (B – H). We analyzed the total area of PSO (Oc+Ot area) and the distance between Oc and Ot (Oc/Ot distance) in order to describe development of the central nervous system. The presence/absence of palps was used as a marker of peripheral nervous system development. The trunk length to width ratio (trunk L/W) and tail length reflect general morphogenesis of the embryo.

The experiments were performed during years 2015 – 2019 in different seasons using wild animals from Sète (Etang de Tau, Mediterranean coast, France). Thus variations in natural animal population in addition to seasonal rearing conditions contributed to variations in morphological parameters of control embryos (Table 2). In order to eliminate the effect of external factors we have compared and normalized each endpoint with the corresponding value in the control group (0.01% DMSO) done on the same day. Statistical analysis was performed on the raw (not-normalized) data using the Kruskal–Wallis test. Analyses were performed at a significance level of 0.01 (for Oc/Ot area, Oc/Ot distance, trunk L/W ratio and tail length) or 0.05 (for % embryos with palps) using STATISTICA v. 13.0 software for Windows. Raw measurements and normalized values are presented in Tables 2 – 5.

In addition, normal, malformed or undevelopped embryos were scored manually. An embryo was considered malformed if the embryo presented signs of antero-posterior elongation (indicating it had undergone gastrulation) or if tadpoles had a crooked tail, an absence of tail, an absence of PSO, or a brain protrusion were observed. Embryos were considered undeveloped if they failed to reach neurula stage (no sign of anteroposterior elongation or gastrulation). We calculated the percentage of: 1) normal embryos [number of normal embryos *100 / (number of normal +

malformed + undeveloped)]; 2) malformed [number of malformed embryos *100 / (number of normal + malformed + undeveloped)]; 3) undeveloped [number of undeveloped embryos *100 / (number of normal + malformed + undeveloped)].

2.5. Genotoxicity assay

Embryos from gastrula to neurula stage were fixed with a fixation solution (4% paraformaldehyde, 0.5 M NaCl in PBS) for 1h at 20°C on a shaker. Then the fixative was removed and embryos were washed twice with PBS. After washing, the samples were incubated in PBS containing 0.1% Triton X-100 and 3% bovine serum albumin (PBSB) for 1h at 20°C on a shaker. The embryos were stained with 1 µg/ml Hoechst in PBSB for 1-2h at 20°C on a shaker. The embryos were either stained with Hoecsht only or double stained with Hoecsht and 4 ng/ml phalloidin in PBSB to observe both DNA and membrane. Double staining was done to ascertain the presence of DNA bridges between two cells and/or multiple nuclei within the same cell. Finally, the embryos were washed twice with PBSB and transferred on a glass slide. The DNA aberrations (multinucleated cells, micronuclei or DNA bridges) were imaged using a confocal Leica SP8 fitted with 40×/1.1NA water objective lens and scored manually. The number of embryos scored in each treatment is shown in Table 6. Embryos were exposed to etoposide 10 µM as a positive control for DNA damage. The relationships between % embryos with DNA aberrations, normal, malformed and undeveloped embryos were quantified according to the Spearman's correlation tests. The t-test was used to establish significance of the correlation between pairs of parameters at a significance level of 0.05.

3. RESULTS

3.1.Morphometric analysis of larval development in untreated embryos

Figure 1 and Table 2 show changes in the morphology of ascidian embryos, scored quantitatively for PSO development (Oc/Ot area, Oc/Ot distance), trunk and tail morphogenesis (trunk L/W ratio, tail length) and qualitatively for palps development (presence of palps). Such morphological changes occur from stage 22 (late tailbud) to stage 26 (hatching larva, see https://www.bpni.bio.keio.ac.jp/chordate/faba/1.4/top.html for staging) (Fig. 1 B-F). At 18 hour-post-fertilization (hpf; stage 22), late tailbud embryos start to pigment their PSO (only one pigmented area = 72 ± 24 μm^2) and no palp is apparent at the anterior tip of the trunk (Fig. 1B). At stage 23, two distinct pigment cells are visible, the otolith (Ot) and the ocellus (Oc) (forming the PSO of an area of 253 ± 64 μm^2; Oc/Ot distance = 18 ± 8 µm) and palps are first visible (Fig. 1C). At stage 24, the pigment cells are separated from each other (the otolith positioned anteriorly and the ocellus posteriorly; Oc/Ot distance = 23 ± 6 µm), and the trunk starts to elongate (Trunk L/W = 1.8 ± 0.3; Fig. 1D). From this stage and up to stage 26, the ocellus and otolith continue to spread and move apart from each other, while the trunk continues to elongate (Fig. 1E, 1F). The tail length only increases until stage 23 and then remains constant (tail length is ~ 500 µm, Table 2). The stage 26 was selected for further analysis of phenotypes induced by exposure to xenobiotics as it is the developmental stage of hatching. At this stage PSO area (mentioned Oc+Ot area in Table 2 and radar charts), PSO distance and tail length reach maximum, palps are fully developed. Later stages are characterized by further trunk elongation, and tail shortening (data not shown, see https://www.bpni.bio.keio.ac.jp/chordate/faba/1.4/top.html). Therefore in further analysis the cultures were fixed and analysed when controls reached stage 26.

3.2. Phenotypes induced by general toxicants

When *Phallusia* embryos are exposed to toxic compounds, deviations from normal embryonic development (i.e. malformations) can be observed as alterations in the quantified endpoints (PSO area and distance, trunk L/W ratio, tail length), compared to untreated control larvae. Images of larval phenotypes are presented in Supplementary Fig. 3. We first analysed the phenotypes induced by exposure to a cytotoxic compound, sodium azide (SA), and to three genotoxicants, etoposide, mitomycin and tributyltin (TBT) (Kirkland et al., 2016) (Table 3, Supplementary figure 3). All four tested chemicals significantly affected all the assessed endpoints, resulting in an embryo resembling a mid tailbud stage embryo (st 22-23, Fig. 1A-D; Supplementary Fig. 3).

Concerning the cytotoxicant, the maximum dose of SA tested (2.5 mM) decreased Oc/Ot distance by 81%, number of embryos with palps by 95%, tail length by 42% and trunk L/W ratio by 43% (Table 3). Exposure to 2.5 mM SA induced 86±14% of malformed, 12±12% normal, and 2±2 undevelopped embryos (Fig. 2). The lowest observed effective concentrations (LOEC) in our study was 1 mM for SA (Tables 1 and 3).

Mitomycin significantly reduced Oc/Ot distance, trunk L/W ratio, and tail length at 10 µM (LOEC) and the percentage of embryos with palps was also reduced at this dose (though $P > 0.01$) (Table 3). At 60 µM, mitomycin strongly affected all endpoints and induced malformations in 91±5% of embryos (Table 3; Supplementary Fig. 3). Exposure to etoposide at concentrations 50 – 75 nM affected PSO area (by 14% at 75 nM), Oc/Ot distance (by 42% at 75 nM), and trunk L/W ratio (by 14% at 75 nM), but had no effect on tail length or on the percentage of embryos with palps (Table 3). At a higher dose of 100 nM, etoposide had an effect similar to SA and mitomycin (60 µM), affecting all studied endpoints (malformation rate 79±16%, Fig. 2). Similarly, TBT at 10 – 20 nM

induced a significant reduction of PSO area (by 40% at 10 nM TBT), of Oc/Ot distance (by 52% at 10 nM TBT), and trunk L/W ratio (by 27% at 10 nM TBT) (Table 3). Exposure to a high dose of TBT (50 nM) also led to severe malformations in general morphology of the larvae, with 82±6% of malformed embryos (Fig. 2; Supplementary Fig. 3).

3.3.*Phenotypes induced by known/suspected EDCs*

Lindane exposure resulted in significant malformations in developing ascidian embryos at 10 µM. This pesticide affected primarily the Oc/Ot distance (62% of control value) and trunk L/W ratio (76% of control value) of ascidian larvae (Table 4, Supplementary Fig. 4). When the concentration of compound was increased to 20 µM, the PSO area decreased to 20% of control value and distance between PSO was 36% of that in control. At 20 µM lindane 53.3±9% of embryos were malformed (Fig. 3).

Similar malformations were observed in atrazine-exposed embryos (Table 4, Supplementary Fig. 4). Our results show that exposure to 25 – 70 µM atrazine induce a small but significant decrease in Oc/Ot distance (to 69% of the control value at 70 µM) and trunk L/W ratio (87% of the control value at 70 µM) without affecting other parameters. Only 12±7% embryos were malformed and 83±7% were normal at 70 µM of atrazine (Fig. 3).

Bisphenol A (BPA), a xenoestrogen, had a very specific effect on ascidian embryos. All tested concentrations of BPA (5 – 10 µM) specifically and significantly reduced PSO pigmentation (PSO area) and Oc/Ot distance (Table 4, Supplementary Fig. 4). The rate of malformed embryos reached 53±8% after exposure to 10 µM BPA with 39±6% normal embryos (Fig. 3).

Chlordane provoked phenotypes similar to lindane, with PSO area (86% of control) and Oc/Ot distance (73 % of control) affected at concentrations of 10 µM (Table 4, Supplementary Fig. 4).

289 The highest tested concentration (50 µM) also decreased the trunk L/W ratio (92% of control), but
290 tail length and palps formation were not significantly affected. Exposure to 50 µM chlordane
291 resulted in 38±6% malformed embryos and 59±7% normal embryos (Fig. 3).

292 A slightly different phenotype was observed after exposure of *Phallusia* embryos to chlorpyrifos
293 (Table 4, Supplementary Fig. 4). Low concentrations 10 – 25 µM affected only Oc+Ot area (85%
294 of the control value) and trunk L/W ratio (89% of the control value). The highest tested
295 concentration (50 µM) induced significant reduction of PSO area (69% of control), Oc/Ot distance
296 (52 % of control), trunk L/W ratio (75% of the control value) and tail length (67% of control), thus
297 affecting also the morphogenesis of the tadpole and not only neural development. Chlorpyrifos at
298 50 µM also induced malformations in 13±7% of exposed embryos (Fig. 3).

299 We have also analyzed the effect of β-Estradiol 3-benzoate (E2B), an ER ligand used in veterinary
300 medicine, on *Phallusia* embryo development. Exposure to E2B did not affect any studied endpoint
301 (Table 4, Fig. 3, Supplementary Fig. 4).

302

303 **3.4. *Phenotypes induced by NR-agonists/antagonists***

304 We then analysed the phenotypes induced by compounds known to specifically bind a vertebrate
305 NR. The RAR agonist all-trans retinoic acid (ATRA) and the RAR antagonist BMS493 both had
306 a strong inhibitory effect on palp development (Table 5, Supplementary Fig. 5). Exposure to 0.1
307 µM ATRA significantly decreased the number of embryos with palps (36% of the control value)
308 without affecting other endpoints. Higher concentrations of ATRA also led to decreased trunk L/W
309 ratio (85% of the control value at 1 µM). A similar phenotype was observed with the RAR inverse

agonist, BMS493, which primarily affected palp development at 3 µM (15% of the control value) and slightly reduced PSO area (87% of the control value) and the tail length (93% of the control).

An RXR antagonist, UVI3003, at 1 µM also significantly affected palps formation (40% of the control value), and reduced PSO area (86% of the control value) (Table 5, Supplementary Fig. 5). Exposure to 2 µM of UVI3003 also led to tail shortening (63% of the control value) and trunk rounding (92% of the control value).

In our study, 4-OHT affected embryo development at concentrations of 5–10 µM (Table 5, Supplementary Fig. 5). At 5 µM 4-OHT reduced mainly the Oc/Ot distance (51 % of control) and the trunk L/W ratio to a lesser extent (83% of the control). At 10 µM tail length was slightly but significantly affected (to 88% of the corresponding control value). In contrast, DES affected *Phallusia* larval development already at 1 µM by reducing PSO area (to 84%), Oc/Ot distance (to 64%) and trunk L/W ratio (to 80% of the corresponding control value; Table 5, Supplementary Fig. 5). At 2 µM all studied endpoints were significantly affected, showing high toxicity of DES to developing ascidian embryos.

Rifampicin exposure significantly affected only Oc/Ot distance (23% of control at 100 µM) and trunk L/W ratio (70% of control at 100 µM; Table 5, Supplementary Fig. 5). Another PXR agonist SR12813 (which was not tested against ascidan PXR) also decreased the distance between PSOs (55% of control at 3 µM) but affected other endpoints such as PSO area (80% of control at 3 µM), and trunk elongation (84% of control at 3 µM) (Table 5, Supplementary Fig. 5). The highest tested concentration (7.5 µM) significantly reduced all studied parameters, thus showing non-specific toxicity.

Embryo exposure to the RORα/γ agonist, SR1078, reduced PSO area (80% of the control value) and trunk L/W ratio (93% of the control value) at 2 µM (Table 5, Supplementary Fig. 5). At 5 µM of SR1078, all studied endpoints except the rate of embryos with palps were significantly reduced, showing nonspecific toxicity of the compound.

Exposure of *Phallusia* embryos to BADGE, a PPAR antagonist, induced a phenotype similar to lindane and atrazine (Table 5, Supplementary Fig. 5). At 1 µM BADGE only the trunk L/W ratio was significantly affected (87% of control value). Higher concentrations of BADGE (2 – 5 µM) further reduced the trunk L/W ratio (to 74% at 5 µM) and affected distance between PSO (to 57% at 5 µM) without affecting the other endpoints.

3.5. Measurement of the genotoxicity induced in ascidian embryos

High concentrations of SA and reference genotoxicants (mitomycin, etoposide, TBT) affect all endpoints in the tadpole larvae (Table 3, Fig. 2), resulting in arrest of development before stage 26. We assessed genotoxicity of these drugs by staining embryo DNA and scoring DNA aberrations. Table 6 and Supplementary Fig. 6 show the scores of DNA aberrations induced by the toxics, after imaging Hoechst-stained *Phallusia* embryos at gastrula and neurula stages.

In the control cultures, embryos showed well aligned nuclei of constant size and tightly packed nuclear DNA in all 50 embryos (Supplementary Fig. 6A). Control cultures also showed more than 80% of normally developed larvae at 22 hpf (stage 26), without major malformations (Fig. 2). Following exposure to 2.5 mM SA we observed appearance of few micronuclei and DNA aberrations in 70% embryos, thus showing that such a dose of SA is genotoxic to ascidian embryos (Table 6; Supplementary Fig. 6B).

353 Similarly to SA-exposed embryos, micronuclei and multinucleated cells were observed in TBT-
354 exposed embryos at 50 nM (Table 6, Supplementary Fig. 6C). In contrast, the embryos exposed to
355 the reference genotoxic compound etoposide (100 nM) exhibited severe DNA damage with
356 formation of DNA bridges in some cells (Table 6, Supplementary Fig. 6D). Exposed embryos were
357 able to develop to tadpole, but showed high rate of malformations (Fig. 2). The higher dose of
358 etoposide (10 µM) also led to formation of DNA bridges, but in the whole embryo (Table 6,
359 Supplementary Fig. 6E). Such embryos developed normally till gastrula stage and did not show
360 any disorganization of cell pattern, the embryo development was blocked shortly after gastrulation
361 (100% undeveloped embryos at 22hpf; Fig. 2). Another reference genotoxic compound,
362 mitomycin C (60 µM), induced formation of DNA bridges in every embryos (Table 6,
363 Supplementary Fig. 6F), but only in parts of the ectoderm (data not shown). Such embryos were
364 still able to develop to the tadpole with 91±5% of malformed and only 8±7% of undeveloped
365 embryos (Fig. 2).

366 We have also assessed whether high concentrations of EDCs (lindane, atrazine, BPA, chlordane,
367 and chlorpyrifos) were genotoxic to ascidian embryos. Most of the pesticides induced little or no
368 DNA damage in *Phallusia* embryos (Table 6). Exposure to 20 µM lindane led to appearance of
369 few micronuclei per gastrula without affecting the pattern of cellular divisions (Supplementary
370 Fig. 6G). This low level of DNA damage is associated with 53.3±9% of malformed embryos (Fig.
371 3). In presence of 70 µM atrazine no DNA aberrations was observed and only 12±7% embryos
372 were malformed (Table 6; Fig. 3). Exposure to 50 µM chlordane resulted in appearance of rare
373 micronuclei (Table 6; Supplementary Fig. 6H) and only 38±6% malformed embryos (Fig. 3).
374 Chlorpyrifos at 50 µM also had low genotoxic effect (Table 6) and induced malformations in

13±7% of exposed embryos (Fig. 3). In the culture treated with 10 µM BPA only 14 out of 119 embryos (11%) were scored as having DNA aberrations (Table 6).

We have also analyzed correlation between the percentage of embryos showing DNA aberrations, with the percentage of normal, malformed and undeveloped embryos (Table 7). According to Spearman's test, the presence of DNA aberrations in *Phallusia* embryos exhibited a strong negative correlation with the percentage of normal embryos in the culture ($r = -0.93$, $p < 0.05$) and showed not significant positive correlations with malformed ($r = 0.5$, $p > 0.05$) and undeveloped embryos ($r = 0.35$, $p > 0.05$).

4. DISCUSSION

We present here a test for developmental toxicity based on larval phenotypes of *Phallusia mammillata* embryos. Previous toxicological studies using ascidian embryos lacked standardized endpoints and protocols for quantification of larval malformations (Dumollard et al., 2017). The teratogenic potential of the tested xenobiotics was assessed by high content analysis of neurodevelopmental endpoints such as pigment sensory organs (PSO) area, distance between ocellus and otolith, rate of embryos with palps, as well as general morphogenesis endpoints such as trunk length/width ratio and tail length. We implemented serial embryonic cultures, imaged and analysed them by scoring quantitative and qualitative endpoints. Transparency of *Phallusia* larvae allows assessment of neurodevelopmental disorders without additional staining. This feature distinguish our model from existing tests on marine invertebrate embryos (Sarkar et al., 2006). Our assay also affords to determine the genotoxic potential of tested compounds in the same cohort of embryos, to correlate genotoxicity with teratogenicity.

Results obtained in the current study show that exposure to toxicants may either induce a phenotype restricted to one or two endpoints or result in malformations resembling a delay in embryonic development (when all endpoints are affected, Supplementary Fig. 3-5). Such delay in embryonic development in response to stress or DNA damage is well described in the literature (Häder et al., 2011; Chiarelli et al., 2019). Therefore phenotypes that show 4 or 5 affected endpoints were considered either non-specific or indicative of DNA damage. The distance between Oc and Ot is the most sensitive endpoint as it was affected by most treatments. The reduction of Oc/Ot distance can be used to determine LOEC values of the compounds. In contrast, specific phenotypes, such as the embryos without palps but with unaffected PSO or tail length, could be characteristic of some toxicants. For example, the rate of embryos with palps is mostly affected

upon exposure to RAR/RXR ligands and the absence of palps may thus be a good indicator of alterations in the RAR/RXR pathway. Conversely, tail length was the least affected parameter demonstrating that tail extension is prevented only at high level of toxicity or in cases of genotoxicity.

4.1. Phenotypes of general toxicants and genotoxicants

Etoposide, mitomycin, and TBT have been shown to induce DNA damage in numerous test systems (reviewed in Kirkland et al., 2016). Our present protocol couples the scoring of DNA aberrations with the morphometric analysis of larval phenotypes, in order to estimate the impact of genotoxicity on teratogenicity. DNA problems can quickly accumulate in ascidian embryos as the early embryo proliferates without an active spindle assembly checkpoint (Chenevert et al., 2020). Therefore, at gastrula and neurula stages DNA aberrations can be easily observed with nuclei staining (in our study with Hoechst). Previous studies on sea urchin (Saotome et al., 1999) and zebrafish (Le Bihanic et al., 2016) showed that mitomycin induced micronuclei formation at concentrations 5 µg/mL and 0.03 µg/mL respectively. In our study, we observed genotoxicity of mitomycin only at 60 µM (20 µg/mL). The longer exposure time in both sea urchin and zebrafish protocols may explain their higher sensitivity. Nevertheless, our approach allowed us to see several types of DNA damage (micronuclei, multinucleated cells, DNA bridges) and correlate them with embryonic phenotypes in a shorter time.

DNA damage was associated with a significant reduction of all studied endpoints. Reduction of all endpoints by SA, TBT, etoposide and mitomycin resulted in phenotypes resembling untreated control embryos at stages 22-23. Interestingly, TBT and SA which are known to have cytotoxic

429 effects (Oyanagi et al., 2015; Weyermann et al., 2005) induced formation of multinucleated cells
430 and micronuclei, whereas clastogenic genotoxicants (mitomycin C and etoposide) led to formation
431 of DNA bridges. Formation of DNA bridges in the whole embryo at gastrula stage led to complete
432 arrest in development (see etoposide 10 µM, Fig. 2).

433 TBT has been shown to affect embryo development in invertebrates (Alzieu, 2000; Gallo, Tosti,
434 2013; Matthiessen, 2019) and to slow down development rate in vertebrates (Bentivegna and
435 Piatkowski, 1998). Bellas et al (2005) found that TBT affects embryo development of the ascidian
436 *Ciona intestinalis* with EC_{50} at 7.1 µg/l (22 nM); our study revealed significant changes in PSO
437 parameters at a similar range of concentrations (10 – 50 nM TBT). Even though no DNA
438 aberrations were observed at 10 nM TBT (data not shown), the teratogenicity of such a dose of
439 TBT was detected as a reduction in PSO area and trunk L/W ratio. Higher concentrations of TBT
440 (50 nM) induced micronuclei and multinucleated cells, demonstrating DNA damage associated
441 with reduction of the ratio of normal embryos in the culture.

442 Previous study have shown that 5 mM SA inhibited myoplasmic reorganization and establishment
443 of anteroposterior axis in embryos of *Ciona intestinalis* (Ishii et al., 2014). In our study, embryos
444 of *Phallusia* were significantly affected by 1 – 2.5 mM SA and DNA damage was observed after
445 exposure to 2.5 mM SA. The phenotypes observed in *Ciona* embryos exposed to 5 mM SA must
446 then be due to the strong genotoxic effect of SA at this dose.

447 Altogether, our observations show that mild DNA damage is reflected in micronuclei at the
448 gastrula/neurula stage and such DNA damage is permissive for development up to stage 23 (TBT,
449 SA). Ascidian embryos can also tolerate appearance of DNA bridges in the epidermis (mitomycin)
450 or in parts of the embryo (etoposide 100 nM). However, extensive DNA damage caused by

accumulation of double strand breaks and formation of DNA bridges throughout the embryo prevents development past stage 10 (gastrula). There was a strong negative correlation between DNA damage and the percentage of normal embryos in the culture. Our study thus allows to speculate that a high percentage of undeveloped embryos is indicative of strong genotoxicity of a tested compound. In contrast observing embryos arrested at stage 22 (and before PSO pigmentation) would indicate medium genotoxicity of the tested compounds. Nevertheless, further studies are needed to confirm this finding.

The highest tested concentrations of xenobiotics (20 µM lindane, 50 µM chlordane, and 50 µM chlorpyrifos, 10 µM BPA) induced formation of micronuclei and the percentage of embryos with DNA problems correlated positively with the percentage of embryos with malformations (Tables 6-7, Fig. 3). However, these concentrations of pesticides induced reduction of at least three studied morphological parameters, but did not lead to the same phenotypes like genotoxicants. Our previous studies showed severe genotoxicity of BPA at 40 µM (Gomes et al., 2019b); however, a small number of embryos with micronuclei was detected already at 10 µM (Table 6). In contrast, atrazine did not induce any detectable DNA damage, and only two endpoints were affected.

Taken together these results suggest that high concentrations of EDCs may induce DNA damage, which severely affects embryo development. However, most of these xenobiotics (lindane, atrazine, chlordane, chlorpyrifos, and BPA) induced embryonic phenotypes at lower concentrations than the ones inducing mild DNA damage, indicating that their main mechanism of action is not related to genotoxicity.

4.2. Phenotypes of EDCs and NRs ligands

473 We compared the phenotypic signature of EDCs with that of known NR ligands because a major
474 mode of action (MoA) of EDCs is via modification of NR activity. The presence of palps was
475 sensitive to RXR and RAR inhibition and activation, but because other NR ligands had overlapping
476 phenotypes it was not possible to find other specific phenotypic signatures.

477 Previous studies have shown that the retinoic acid (RA) signaling pathway regulates axial
478 patterning and neurogenesis in the developing central and peripheral nervous systems of chordates
479 including ascidians (Fujiwara and Kawamura, 2003; Nagatomo et al., 2003; Zieger et al., 2018).
480 RA signal is mediated by an RA-binding heterodimeric transcription factor consisting of RAR and
481 RXR (Mangelsdorf and Evans, 1995). Both receptors are expressed in neurogenic domains of
482 ascidian embryos (Nagatomo et al., 2003, Gomes et al., 2019a), thus their ligands can most likely
483 affect ascidian larval brain formation (Nagatomo et al., 2003). In the current study we analyzed
484 the effect of the RAR agonist all-trans retinoic acid (ATRA), of the RAR antagonist BMS493 and
485 of the RXR antagonist UVI3003, on *Phallusia* embryos. All compounds completely blocked
486 formation of the adhesive palps and slightly but consistently increased the distance between PSO.
487 These results are in agreement with previous studies (Dumollard et al., 2017; Nagatomo et al.,
488 2003) showing similar phenotypes in ascidian embryos treated with ATRA. The similar
489 phenotypes induced by activation and inactivation of RAR can be explained by a downregulation
490 of RA metabolism in ATRA-exposed tailbud embryo (Nagatomo et al., 2003) as found in the
491 mouse (Lee at al., 2012) but this hypothesis should be confirmed in ascidians.

492 The RAR-orphan receptor (ROR) is ubiquitously expressed from the 16-cell to the tailbud stage
493 (Gomes et al., 2019a). In the tadpole, ROR expression is observed in the anterior region adjacent
494 to the brain, suggested to give rise to the future oral siphon in the adult (Gomes et al., 2019a;
495 Tolkin and Christiaen, 2016; Veeman et al., 2010). The ROR agonist SR1078 slightly reduced

PSO area and trunk L/W ratio at 2 µM, whereas higher concentration affected almost all studied endpoints (except tail length), indicating non-specific toxicity. This suggests that ROR might participate in PSO development but this should be confirmed by specific ROR knockdown.

It is known that the vertebrate pregnane X receptor (PXR) is a member of the NR super-family which regulates transcription of genes involved in the metabolism and excretion of endogenous and exogenous toxic compounds (Fidler et al., 2012). PXR transcriptional targets in mammals include the cytochrome P450 (CYP) 2C and 3A enzymes, and transporters such as multidrug resistant protein (MDR, ABCB1) (Reschly et al., 2007). Those proteins in turn regulate, transport and metabolize xenobiotics, steroid hormones, and vitamins. In ascidians, such as *Ciona intestinalis* and *Phallusia mammillata*, genome encodes an orthologue of the vertebrate PXR and vitamin D receptor (VDR), denoted VDR/PXR (Yagi et al., 2003). Our previous study indicate that, in *Phallusia*, VDR/PXR is expressed in the brain region of embryos and larvae (Gomes et al., 2019a). As predicted, the current study shows significant changes in PSO development and trunk elongation after exposure to lindane and chlordane (PXR ligands according to Lemaire et al., 2004), and PXR agonists (rifampicin and SR12813). Functional inactivation of PXR in ascidians is now required to confirm the role of PXR in PSO development and trunk elongation.

Ascidians possess a single copy of the PPAR gene (Yagi et al., 2003), which is expressed in few cells within the ascidian brain, in the vicinity of the PSO (Gomes et al., 2019a). Interestingly, a synthetic ligand of PPARγ, BADGE (Wright et al., 2000), showed significant effect on PSO development at 1 – 5 µM. Similar cocnentrations of BADGE also caused neurodevelopmental toxicity in an amphibian (*Rhinella arenarum*, EC_{50} = 0.5 µM) (Hutler et al., 2016).

The majority of EDCs act primarily via steroid receptors (UNEP/WHO, 2013) but ascidians lack steroid binding nuclear receptors such as ER or AR (Yagi et al., 2003). As expected, estradiol benzoate (which binds only ER) was not toxic to ascidian embryos. The xenoestrogens DES, 4OHT and BPA all inhibited PSO development potentially via inhibition of the estrogen related receptor (ERR) which is expressed in the PSO of the ascidian larva (Gomes et al., 2019b). Indeed, even though ERR is an orphan NR, synthetic molecules such as DES and 4-OHT can directly bind ascidian (Park et al., 2009) and vertebrate ERRs (Coward et al., 2001, Gibert et al., 2011), while BPA binds vertebrate ERRγ (Tohmé et al., 2014). Furthermore, ERR plays important roles in the development of the vertebrate brain and sensory organs (Hermans-Borgmeyer et al., 2000; Lim et al., 2015; Chen and Nathans, 2007). Together, our observations suggest that ERR is involved in ascidian larval brain formation (see also Gomes et al., 2019b). The xenobiotics targeting ERR (such as BPA, DES or 4OHT) are predicted to exert neurodevelopmental toxicity in ascidians. However, since PSO development was affected also by other EDCs and other NR ligands, further studies should clarify the role of ERR in PSO development.

5. CONCLUSION

Overall we conclude that *Phallusia mammillata* is a suitable and sensitive model for toxicity screening. The ability to easily assess neural development in the transparent *Phallusia* larva also offers to assess the impact on neurodevelopment of sublethal concentrations of toxicants shedding light on potential mechanisms of teratogenicity or mode of actions of toxicants. The proposed embryo/larval assay allows a fast and quantitative evaluation of teratogenic effects of xenobiotics on ascidian embryo and a correlation with the extent of genotoxicity.

539 Analysis of embryo phenotypes induced by different compounds indicate that severe
540 malformations resembling developmental delay are associated with genotoxicity. In contrast,
541 compounds like EDCs and NR ligands are impacting mostly neurodevelopmental endpoints. This
542 study sets the stage for quantitative analysis of embryo phenotypes that could be used to study not
543 only the teratogenicity of NR-targeting EDCs, but also the potential effects of pollutants that can
544 be dissolved in sea water.

545 Functional studies are needed to characterize *Phallusia* embryonic phenotypes observed after
546 activation or inhibition of NRs, and consequently compare these phenotypes with phenotypes
547 induced by a library of compounds, as a first step for performing predictive toxicology on marine
548 invertebrate organisms.

549

550 **Declaration of interest**

551 We declare that we have no financial or non-financial competing interests.

552

553 **Acknowledgements**

554 The authors would like to thank Laurent Gilletta from LBDV and the service aquariologie of
555 Centre de Ressources Biologiques of the Institut de la Mer de Villefranche (CRB - IMEV) that is
556 supported by EMBRC-France, and France BioImaging whose French state funds are managed by
557 the Agence Nationale de la Recherche (ANR) within the “Investissement d’Avenir” program
558 (ANR-10-INBS-02). The experiments reported in this study were financed by an ANR grant
559 (Marine-EmbryoTox project, ANR-14-OHRI-0009-01-1). Isa Gomes was funded by the French

Ministry of Higher Education, of Research and Innovation and Doctoral School "Life Science Complexity" (ED515) for PhD scholarship. Ievgeniia Gazo thanks to the Ministry of Education, Youth and Sports of the Czech Republic: the CENAKVA project (LM2018099); project Reproductive and Genetic Procedures for Preserving Fish Biodiversity and Aquaculture (CZ.02.1.01/0.0/0.0/16_025/0007370), and the Czech Science Foundation GAČR 19-11140Y.

REFERENCES

Alzieu, C., 2000. Impact of tributyltin on marine invertebrates. Ecotoxicol. 9, 71-76.

Battistoni, M., Mercurio, S., Ficetola, G.F., Metruccio, F.C., Menegola, E., Pennati, R., 2018. The Ascidian Embryo Teratogenicity assay in Ciona intestinalis as a new teratological screening to test the mixture effect of the co-exposure to ethanol and fluconazole. Environ. Toxicol. Pharmacol. 57, 76-85. doi: 10.1016/j.etap.2017.11.014.

Bellas, J., Beiras, R., Mariño-Balsa, J.C., Fernández, N., 2005. Toxicity of organic compounds to marine invertebrate embryos and larvae: a comparison between the sea urchin embryogenesis bioassay and alternative test species. Ecotoxicol., 14(3), 337-353.

Bentivegna, C.S., Piatkowski, T., 1998. Effects of tributyltin on medaka (Oryzias latipes) embryos at different stages of development. Aquat. Toxicol. 44, 117–128.

Castro, L.F., Lima, D., Machado, A., Melo, C., Hiromori, Y., Nishikawa, J., Nakanishi, T., Reis-Henriques, M.A., Santos, M.M., 2007. Imposex induction is mediated through the Retinoid X Receptor signalling pathway in the neogastropod Nucella lapillus. Aquat. Toxicol. 85(1), 57-66.

Chen, J., Nathans, J., 2007. Estrogen-Related Receptor β/NR3B2 controls epithelial cell fate and endolymph production by the Stria Vascularis. Dev. Cell 13, 325–337. doi 10.1016/j.devcel.2007.07.011.

Chenevert, J., Roca, M., Besnardeau, L., Ruggiero, A., Nabi, D., McDougall, A., Copley, R.R., Christians, E., Castagnetti S., 2020. The spindle assembly checkpoint functions during early development in non-chordate embryos. Cells 9(5), E1087. doi: 10.3390/cells9051087.

Chiarelli, R., Martino, C., Roccheri, M.C., 2019. Cadmium stress effects indicating marine pollution in different species of sea urchin employed as environmental bioindicators. Cell Stress Chaperones 24(4), 675-687. doi: 10.1007/s12192-019-01010-1.

Coward, P., Lee, D., Hull, M.V., Lehmann, J.M., 2001. 4-Hydroxytamoxifen binds to and deactivates the estrogen-related receptor gamma. Proc. Natl. Acad. Sci. USA 98(15), 8880-4.

591 Delsuc, F., Brinkmann, H., Chourrout, D., Philippe, H., 2006. Tunicates and not
592 cephalochordates are the closest living relatives of vertebrates. Nature 439(7079), 965-968.

593 Desbiolles, F., Malleret, L., Tiliacos, C., Wong-Wah-Chung, P., Laffont-Schwob, I., 2018.
594 Occurrence and ecotoxicological assessment of pharmaceuticals: Is there a risk for the
595 Mediterranean aquatic environment? Sci. Total. Environ. 639, 1334-1348. doi:
596 10.1016/j.scitotenv.2018.04.351.

597 Dixon, D.R., Pruski, A.M., Dixon L.R.J., Jha, A.N., 2002. Marine invertebrate eco-
598 genotoxicology: a methodological overview. Mutagenesis 17 (6), 495–507.

599 Dumollard, R., Gazo, I., Gomes, I.D.L., Besnardeau, L., McDougall, A., 2017. Ascidians: An
600 Emerging Marine Model for Drug Discovery and Screening. Curr. Top. Med. Chem. 17(18),
601 2056-2066. doi: 10.2174/1568026617666170130104922.

602 Ekins, S., Reschly, E.J., Hagey, L.R., Krasowski, M.D., 2008. Evolution of pharmacologic
603 specificity in the pregnane X receptor. BMC Evol. Biol. 8, 103. doi: 10.1186/1471-2148-8-
604 103.

605 Esner, M., Meyenhofer, F., Bickle, M., 2018. Live-cell high content screening in drug
606 development. Methods Mol. Biol. 1683, 149-164. doi: 10.1007/978-1-4939-7357-6_10.

607 Fidler, A.E., Holland, P.T., Reschly, E.J., Ekins, S., Krasowski, M.D., 2012. Activation of a
608 tunicate (Ciona intestinalis) xenobiotic receptor orthologue by both natural toxins and synthetic
609 toxicants. Toxicon. 59(2), 365-372. doi: 10.1016/j.toxicon.2011.12.008.

610 Fujiwara, S., Kawamura, K., 2003. Acquisition of retinoic acid signaling pathway and
611 innovation of the chordate body plan. Zool. Sci. 20, 809-818.

612 Gallo, A., Tosti, E., 2013. Adverse effect of antifouling compounds on the reproductive
613 mechanisms of the ascidian Ciona intestinalis. Mar. Drugs, 11(9), 3554-3568.
614 https://doi.org/10.3390/md11093554

615 Gallo, A., Tosti, E., 2015. The ascidian Ciona intestinalis as model organism for
616 ecotoxicological bioassays. J. Marine Sci. Res. Dev. 5, e138. doi:10.4172/2155-
617 9910.1000e138

618 Gibert, Y., Sassi-Messai, S., Fini, J.B., Bernard, L., Zalko, D., Cravedi, J.P., Balaguer, P.,
619 Andersson-Lendahl, M., Demeneix, B., Laudet, V., 2011. Bisphenol A induces otolith
620 malformations during vertebrate embryogenesis. BMC Dev. Biol. 11, 4. doi: 10.1186/1471-
621 213X-11-4.

622 Gomes, I.D.L., Gazo, I., Besnardeau, L., Hebras, C., McDougall, A., Dumollard, R., 2019a.
623 Potential roles of nuclear receptors in mediating neurodevelopmental toxicity of known
624 endocrine-disrupting chemicals in ascidian embryos. Mol. Reprod. Dev. 86, 1333–1347. doi:
625 10.1002/mrd.23219.

Gomes, I.D.L., Gazo, I., Nabi, D., Besnardeau, L., Hebras, C., McDougall, A., Dumollard R., 2019b. Bisphenols disrupt differentiation of the pigmented cells during larval brain formation in the ascidian. Aquat. Toxicol. 216, 105314. doi: 10.1016/j.aquatox.2019.

Häder, D.P., Helbling, E.W., Williamson, C.E., Worrest, R.C., 2011. Effects of UV radiation on aquatic ecosystems and interactions with climate change. Photochem. Photobiol. Sci. 10, 242-260.

Hermans-Borgmeyer, I., Süsens, U., Borgmeyer, U., 2000. Developmental expression of the estrogen receptor-related receptor gamma in the nervous system during mouse embryogenesis. Mech. Dev. 97(1-2), 197-199.

Holland, L.Z., Holland, N.D., 1999. Chordate origins of the vertebrate central nervous system. Curr. Opin. Neurobiol. 9(5), 596-602.

Hudson, C., 2016. The central nervous system of ascidian larvae. Wiley. Interdiscip. Rev. Dev. Biol. 5(5), 538-561. doi: 10.1002/wdev.239.

Hutler, W.I., Svartz, G.V., Aronzon, C.M., Pérez Coll, C., 2016. Developmental toxicity of bisphenol A diglycidyl ether (epoxide resin badge) during the early life cycle of a native amphibian species. Environ. Toxicol. Chem. 35, 3031-3038. doi:10.1002/etc.3491.

Ishii, H., Shirai, T., Makino, C., Nishikata, T., 2014. Mitochondrial inhibitor sodium azide inhibits the reorganization of mitochondria-rich cytoplasm and the establishment of the anteroposterior axis in ascidian embryo. Dev. Growth. Differ. 56(2), 175-188. doi: 10.1111/dgd.12117.

Kanda, M., Wada, H., Fujiwara, S., 2009. Epidermal expression of Hox1 is directly activated by retinoic acid in the Ciona intestinalis embryo. Dev. Biol. 335(2), 454-463. doi: 10.1016/j.ydbio.2009.09.027.

Kirkland, D., Kasper, P., Martus, H. J., Müller, L., van Benthem, J., Madia, F., Corvi, R., 2016. Updated recommended lists of genotoxic and non-genotoxic chemicals for assessment of the performance of new or improved genotoxicity tests. Mutat. Res. Genet. Toxicol. Environ. Mutagen. 795, 7 – 30.

Le Bihanic, F., Di Bucchianico, S., Karlsson, H.L., Dreij, K., 2016. In vivo micronucleus screening in zebrafish by flow cytometry. Mutagenesis 31(6), 643–653.

le Maire, A., Grimaldi, M., Roecklin, D., Dagnino, S., Vivat-Hannah, V., Balaguer, P., Bourguet, W., 2009. Activation of RXR-PPAR heterodimers by organotin environmental endocrine disruptors. EMBO Rep. 10, 367–373.

Lee, L.M., Leung, C.Y., Tang, W.W., Choi, H.L., Leung, Y.C., McCaffery, P.J., Wang, C.C., Woolf, A.S., Shum, A.S., 2012. A paradoxical teratogenic mechanism for retinoic acid. Proc. Natl. Acad. Sci. USA 109(34), 13668-13673. doi: 10.1073/pnas.1200872109.

Lemaire, G., de Sousa, G., Rahmani, R., 2004. A PXR reporter gene assay in a stable cell culture system: CYP3A4 and CYP2B6 induction by pesticides. Biochem. Pharmacol. 68(12), 2347-2358.

Lim, J., Choi, H.S., Choi, H.J., 2015. Estrogen-related receptor gamma regulates dopaminergic neuronal phenotype by activating GSK3β/NFAT signaling in SH-SY5Y cells. J Neurochem. 133(4), 544-557. doi: 10.1111/jnc.13085.

Mangelsdorf, D.J., Evans, R.M., 1995. The RXR heterodimers and orphan receptors. Cell 83, 841-850

Matsushima, A., Ryan, K., Shimohigashi, Y., Meinertzhagen, I.A., 2013. An endocrine disruptor, bisphenol A, affects development in the protochordate Ciona intestinalis: hatching rates and swimming behavior alter in a dose-dependent manner. Environ. Pollut. 173, 257-263. doi: 10.1016/j.envpol.2012.10.015.

Matthiessen, P., 2019. The impact of organotin pollution on aquatic invertebrate communities – are molluscs the only group whose populations have been affected? Env. Sci. Heal. 11, 13-20. doi: 10.1016/j.coesh.2019.06.003

Mnif, W., Hassine, A.I., Bouaziz, A., Bartegi, A., Thomas, O., Roig, B., 2011. Effect of endocrine disruptor pesticides: a review. Int. J. Environ. Res. Public Health. 8(6), 2265-2303. doi: 10.3390/ijerph8062265.

Nagatomo, K., Ishibashi, T., Satou, Y., Satoh, N., Fujiwara, S., 2003. Retinoic acid affects gene expression and morphogenesis without upregulating the retinoic acid receptor in the ascidian Ciona Intestinalis. Mech. Dev.120 (3), 363‑372.

Nishikawa, J., Mamiya, S., Kanayama, T., Nishikawa, T., Shiraishi, F., Horiguchi, T., 2004. Involvement of the retinoid X receptor in the development of imposex caused by organotins in gastropods. Environ. Sci. Technol. 38(23), 6271-6276.

OECD (2016), Test No. 473: In Vitro Mammalian Chromosomal Aberration Test, OECD Guidelines for the Testing of Chemicals, Section 4, OECD Publishing, Paris, https://doi.org/10.1787/9789264264649-en.

OECD (2016), Test No. 487: In Vitro Mammalian Cell Micronucleus Test, OECD Guidelines for the Testing of Chemicals, Section 4, OECD Publishing, Paris, https://doi.org/10.1787/9789264264861-en.

OECD (2016), Test No. 489: In Vivo Mammalian Alkaline Comet Assay, OECD Guidelines for the Testing of Chemicals, Section 4, OECD Publishing, Paris, https://doi.org/10.1787/9789264264885-en.

Oyanagi, K., Tashiro, T., Negishi, T., 2015. Cell-type-specific and differentiation-status-dependent variations in cytotoxicity of tributyltin in cultured rat cerebral neurons and astrocytes. J. Toxicol. Sci. 40(4), 459-468. doi: 10.2131/jts.40.459.

Park, W., Kim, G.J., Choi, H.S., Vanacker, J.M., Sohn, Y.C., 2009. Conserved properties of a urochordate estrogen receptor-related receptor (ERR) with mammalian ERRalpha. Biochim. Biophys. Acta. 1789(2), 125-134. doi: 10.1016/j.bbagrm.2008.08.011.

Reschly, E.J., Bainy, A.C., Mattos, J.J., Hagey, L.R., Bahary, N., Mada, S.R., Ou, J., Venkataramanan, R., Krasowski, M.D., 2007. Functional evolution of the vitamin D and pregnane X receptors. BMC Evol. Biol. 7, 222.

Saotome, K., Sofuni, T., Hayashi, M., 1999. A micronucleus assay in sea urchin embryos. Mutat. Res. 446(1), 121-127.

Sardet, C., McDougall, A., Yasuo, H., Chenevert, J., Pruliere, G., Dumollard, R., Hudson, C., Hebras, C., Le Nguyen, N., Paix, A., 2011. Embryological methods in ascidians: the Villefranche-sur-Mer protocols. Methods Mol. Biol. 770, 365-400.

Sarkar, A., Ray, D., Shrivastava, A.N., Sarker, S., 2006. Molecular Biomarkers: their significance and application in marine pollution monitoring. Ecotoxicology 15(4), 333-340. doi:10.1007/s10646-006-0069-1.

Takamura, K., 1998. Nervous network in larvae of the ascidian Ciona intestinalis. Dev. Genes. Evol. 208, 1–8.

Tohmé, M., Prud'homme, S.M., Boulahtouf, A., Samarut, E., Brunet, F., Bernard, L., Bourguet, W., Gibert, Y., Balaguer, P., Laudet, V., 2014. Estrogen-related receptor γ is an in vivo receptor of bisphenol A. FASEB J. 28(7), 3124-3133. doi: 10.1096/fj.13-240465.

Tolkin, T., Christiaen, L., 2016. Rewiring of an ancestral Tbx1/10-Ebf-Mrf network for pharyngeal muscle specification in distinct embryonic lineages. Development 143(20), 3852–3862. https://doi.org/10.1242/dev.136267

UNEP/WHO, 2013. World Health Organization, United Nations Environment Programme (WHO-UNEP). In: Bergman, A., Heindel, J.J., Jobling, S., Kidd, K.A., Zoeller, R.T. (Eds.), State of the Science of Endocrine Disrupting Chemicals. Available at: http://www.who.int/ceh/publications/endocrine/en/index.htm.

Urushitani, H., Katsu, Y., Kagechika, H., Sousa, A.C.A., Barroso, C.M., Ohta, Y., Shiraishi, H., Iguchi, T., Horiguchi, T. 2018. Characterization and comparison of transcriptional activities of the retinoid X receptors by various organotin compounds in three prosobranch gastropods; Thais clavigera, Nucella lapillus and Babylonia japonica. Aquat. Toxicol. 199, 103-115. doi: 10.1016/j.aquatox.2018.03.029.

Veeman, M.T., Newman-Smith, E., El-Nachef, D., Smith, W.C., 2010. The ascidian mouth opening is derived from the anterior neuropore: Reassessing the mouth/neural tube relationship in chordate evolution. Dev. Biol. 344(1), 138–149. https://doi.org/10.1016/j.ydbio.2010.04.028

Weyermann, J., Lochmann, D., Zimmer, A., 2005. A practical note on the use of cytotoxicity assays. Int. J. Pharm. 288(2), 369-376.

734 Wright, H.M., Clish, C.B., Mikami, T., Hauser, S., Yanagi, K., Hiramatsu, R., Serhan, C.N.,
735 Spiegelman, B.M., 2000. A synthetic antagonist for the peroxisome proliferator-activated
736 receptor gamma inhibits adipocyte differentiation. J. Biol. Chem. 275(3), 1873-1877.

737 Yagi, K., Satou, Y., Mazet, F., Shimeld, S.M., Degnan, B., Rokhsar, D., Levine, M., Kohara,
738 Y., Satoh, N., 2003. A genomewide survey of developmentally relevant genes in Ciona
739 intestinalis. III. Genes for Fox, ETS, nuclear receptors and NFkappaB. Dev. Genes Evol. 213,
740 235–244. doi 10.1007/s00427-003-0322-z.

741 Yamada, A., Nishida, H., 2014. Control of the number of cell division rounds in distinct tissues
742 during ascidian embryogenesis. Dev. Growth Differ. 56(5), 376-386. doi: 10.1111/dgd.12141.

743 Zega, G., Pennati, R., Candiani, S., Pestarino, M., De Bernardi, F., 2009. Solitary ascidians
744 embryos (Chordata, Tunicata) as model organisms for testing coastal pollutant toxicity.
745 Inverteb. Surv. J., 6(1 (Suppl)), S29-S34.

746 Zieger, E., Garbarino, G., Robert, N.S.M., Yu, J.K., Croce, J.C., Candiani, S., Schubert, M.,
747 2018. Retinoic acid signaling and neurogenic niche regulation in the developing peripheral
748 nervous system of the cephalochordate amphioxus. Cell Mol. Life Sci. 75(13), 2407-2429. doi:
749 10.1007/s00018-017-2734-3.

750

Table 1. List of chemicals used for toxicity screening and concentrations analyzed in the current study, listed in the order presented on figures 2 - 4. The LOEC is the lowest tested concentration (experimental) that is significantly different from the control as determined by one or several endpoints (Kruskal-Wallis test, $P < 0.05$). Last column mention the affected endpoint at LOEC.

Chemical name	**Doses assessed in the current study**	**LOEC[1]**	**Affected endpoints at LOEC**
Sodium azide	0.1 – 2.5mM	1 mM	PSO[2] area, PSO distance, Trunk L/W ratio[3], Tail length
Tributyltin	10 – 50 nM	10 nM	PSO area, PSO distance, Trunk L/W ratio
Etoposide	50 nM – 10 µM	50 nM	PSO area, PSO distance, Trunk L/W ratio
Mitomycin C	10 – 60 µM	10 µM	PSO distance, Trunk L/W ratio, Tail length
γ-BHC (Lindane)	2.5 – 20 µM	10 µM	PSO distance, Trunk L/W ratio
Atrazine	1 – 70 µM	50 µM	PSO distance, Trunk L/W ratio
Bisphenol A (BPA)	1 – 50 µM	1 µM (Gomes et al., 2019b)	PSO area, PSO distance
cis/trans-Chlordane	10 - 50 µM	10 µM	PSO area, PSO distance
Chlorpyrifos	10 – 100 µM	10 µM	PSO area
Estradiol benzoate (E2B)	5 – 10 µM	ND[4]	ND[4]

ATRA (all trans retinoic acid)	0.01 – 5 µM	0.1 µM	% embryos with palps, Trunk L/W ratio
BMS493	1 – 5 µM	3 µM	PSO area, % embryos with palps, Tail length
UVI3003	0.1 – 2 µM	1 µM	PSO area, % embryos with palps
4-Hydroxytamoxifen (4HT)	1 – 50 µM	5 µM	PSO distance
Diethylstilbestrol (DES)	0.1 – 25 µM	1 µM	PSO area, PSO distance, Trunk L/W ratio
Rifampicin	10 – 100 µM	50 µM	PSO distance, Trunk L/W ratio
SR 1078	0.1 – 5 µM	2 µM	PSO area
BADGE	1 – 100 µM	1 µM	Trunk L/W ratio
SR 12813	1.5 – 10 µM	3 µM	PSO area, PSO distance, Trunk L/W ratio

[1] LOEC - the lowest tested concentration (experimental) that is significantly different from the control as determined by one or several endpoints (Kruskal-Wallis test, $P < 0.05$).

[2] PSO – pigmented sensory organs

[3] Trunk L/W ratio – trunk length / width ratio

[4] ND – not determined

Figure 1. Changes of morphological parameters during embryonic development (between stage 22 and stage 26). **A.** The measured endpoints are summarized in the radar chart depicting normalized values (normalized to stage 26 values): ocellus (Oc) + otolith (Ot) area (μm^2); Oc/Ot distance (μm); percentage of embryos with palps (%); trunk L/W (length/width) ratio; tail length (μm). Measurement of all parameters was performed for min N=50 embryos. Asterisks indicate significant difference compared to the control (Kruskal-Wallis test, $P < 0.05$). **B.** Trunk region at 18 hpf (stage 22). Black arrow shows formation of ocellus (Oc). **C.** Trunk region at 19 hpf (stage 23). Black arrow shows formation of ocellus (Oc), dark grey arrow shows formation of otolith (Ot) and separation of two pigmented sensory organs (PSO) at stage 23. White arrow indicates formation of palps at stage 23 **D.** Trunk region at 20 hpf (stage 24). **E.** Trunk region at 21 hpf (stage 25). **F.** Trunk region at 22 hpf (stage 26). Scale bars correspond to 20 μm

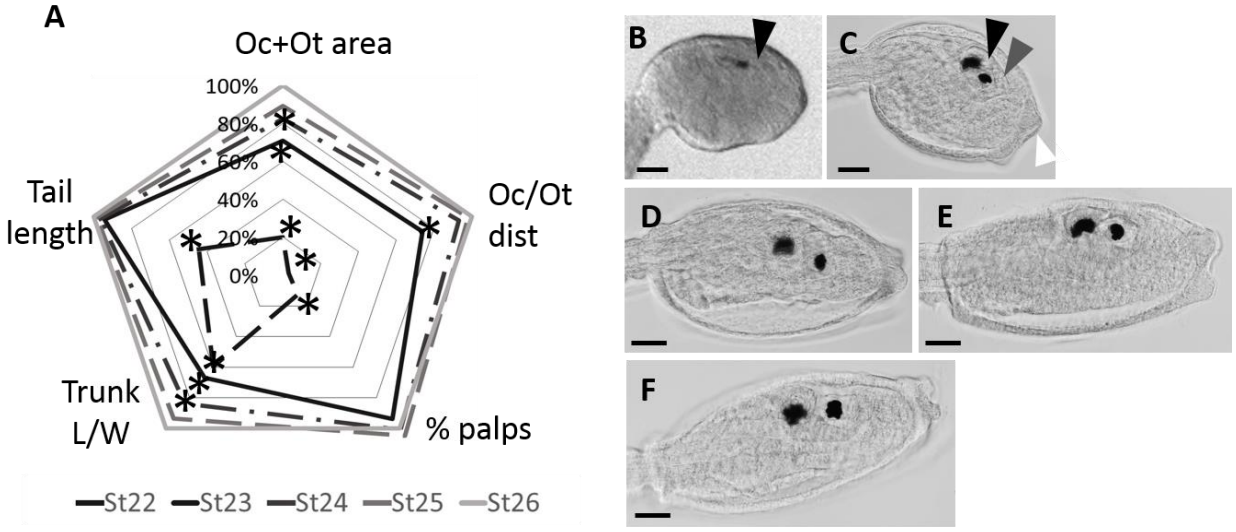

Table 2. Changes of morphological parameters during embryonic development. (between stage 22 and stage 26). The mean values ± SD are presented. N is the number of embryos assessed at each stage. The line "St26 controls-2015-209" shows average values of morphological parameters from all cultures performed in this study.

Stage of embryo development	N	PSO area, μm^2	PSO distance, μm	Palps, %[1]	Trunk L/W ratio[2]	Tail length, μm
Stage 22	49	72 ± 24	0,8 ± 3	12	1,3 ± 0,1	237 ± 24
Stage 23	47	253 ± 64	18 ± 8	89	1,4 ± 0,1	506 ± 37
Stage 24	49	294 ± 47	23 ± 6	96	1,8 ± 0,3	516 ± 173
Stage 25	46	317 ± 41	24 ± 4	100	1,9 ± 0,2	527 ± 146
Stage 26	75	320 ± 47	24 ± 7	100	2 ± 0,2	535 ± 116
Stage 26, controls 2015-2019	4903	292 ±142	20 ± 11	92 ± 3.2	2.6 ± 1.5	483 ± 162

[1]Palps, % – the percentage embryos with palps;

[2]Trunk L/W ratio – trunk length / width ratio

Table 3. Morphometric analysis of phenotypes observed in *Phallusia mammillata* larvae exposed to toxicants. N shows the number of embryos analyzed. The table summarize the following endpoints: ocellus (Oc) + otolith (Ot) area (µm2); Oc/Ot distance (µm); percentage of embryos with palps (%); trunk L/W (length/width) ratio; tail length (µm). All measurements are performed at 22 hpf. Data presented as means ± S.E and as % to the control. Asterisks indicate significant difference compared to the control (Kruskal-Wallis test, $P < 0.05$). SA indicate sodium azide ; TBT – tributyltin.

Treatment	N	Oc/Ot area, μm^2, mean ± S.E.	Oc/Ot area, % to the control	Oc/Ot distance, µm, mean ± S.E.	Oc/Ot distance % to the control	% palps, means ± S.E.	Palps% to the control	Trunk L/W ratio, means ± S.E.	Trunk L/W % to the control	Tail length, µm, means ± S.E.	Tail length % to the control
control	322	362.9 ± 8.1	-	19.7 ± 0.6	-	91.7 ± 3.2	-	2.3 ± 0.03	-	550.1 ± 4.6	-
SA 100uM	317	355.3 ± 8.6	93%	19.4 ± 0.6	95%	90.1 ± 2.9	100%	2.3 ± 0.03	94%	531.1 ± 4.7	97%
SA 1mM	151	**268 ± 16.6 ***	**58%**	**10.1 ± 0.9 ***	**37%**	35.6 ± 31.5	37%	**1.7 ± 0.03 ***	**67%**	**425.3 ± 18.6 ***	**66%**
SA 2.5mM	115	**300.2 ± 19.2 ***	**56%**	**4.1 ± 0.9 ***	**19%**	**3.8 ± 3.8 ***	**6%**	**1.2 ± 0.01 ***	**57%**	**339.2 ± 11.2 ***	**58%**
control	120	314.1 ± 12.4	-	21.7 ± 1.1	-	93.7 ± 3.7	-	2.2 ± 0.04	-	510.9 ± 12.2	-
TBT 10nM	106	**186.8 ± 13.5 ***	**60%**	**10.5 ± 1.2 ***	**48%**	66.1 ± 14.5	72%	**1.6 ± 0.05 ***	**73%**	477.7 ± 14.1	99%
TBT 20nM	133	**164.3 ± 12.1 ***	**47%**	**9.4 ± 1 ***	**38%**	46.4 ± 17.3	50%	**1.6 ± 0.05 ***	**70%**	443.6 ± 13.3	79%
TBT 50nM	122	**40.8 ± 7.5 ***	**10%**	**1.2 ± 0.5 ***	**4%**	**13.3 ± 12.3 ***	**14%**	**1.3 ± 0.03 ***	**54%**	**302.3 ± 13.3 ***	**49%**
control	211	298.1 ± 6.5	-	25.6 ± 0.6	-	98.8 ± 1.2	-	2.2 ± 0.02	-	433.8 ± 18.8	-
Etoposide 50nM	168	**252.4 ± 6.3 ***	**95%**	**21.3 ± 0.8 ***	**80%**	98.8 ± 0.6	100%	**2 ± 0.02 ***	**92%**	428.9 ± 20.3	97%
Etoposide 75nM	116	**221.3 ± 7.4 ***	**86%**	**14.6 ± 1.1 ***	**58%**	70.9 ± 16.9	73%	**1.7 ± 0.03 ***	**86%**	463.7 ± 19.2	92%
Etoposide 100nM	139	**120.8 ± 7.7 ***	**44%**	**4.2 ± 0.7 ***	**18%**	**20.1 ± 18.7 ***	**21%**	**1.3 ± 0.02 ***	**63%**	**253.2 ± 16.1 ***	**56%**
control	410	366.3 ± 5.4	-	20.6 ± 0.5	-	93.6 ± 1.5	-	2.4 ± 0.01	-	443.9 ± 1.5	-
Mitomycin C 10µM	361	340.8 ± 6.7	95%	**15.7 ± 0.7 ***	**81%**	56.5 ± 11.7	41%	**1.5 ± 0.01 ***	**56%**	**317.4 ± 4.7 ***	**93%**
Mitomycin C 40µM	284	285.6 ± 10.3	96%	**10.3 ± 1 ***	**44%**	**12.4 ± 6.2 ***	**15%**	**1.3 ± 0.01 ***	**46%**	**234.4 ± 5.8 ***	**71%**
Mitomycin C 60µM	165	**226 ± 13.4 ***	**62%**	**4.4 ± 0.9 ***	**32%**	**0.3 ± 0.3 ***	**0%**	**1.2 ± 0.01 ***	**44%**	**421.5 ± 2.6 ***	**59%**

Figure 2. The percentage of normal (light grey), malformed (dark grey) and undeveloped (black) embryos in the sodium azide (SA) 2.5 mM, etoposide (Et) 100 nM and 10 µM, mitomycin 60 µM, tributyltin (TBT) 50 nM. Data are presented as means ± SEM.

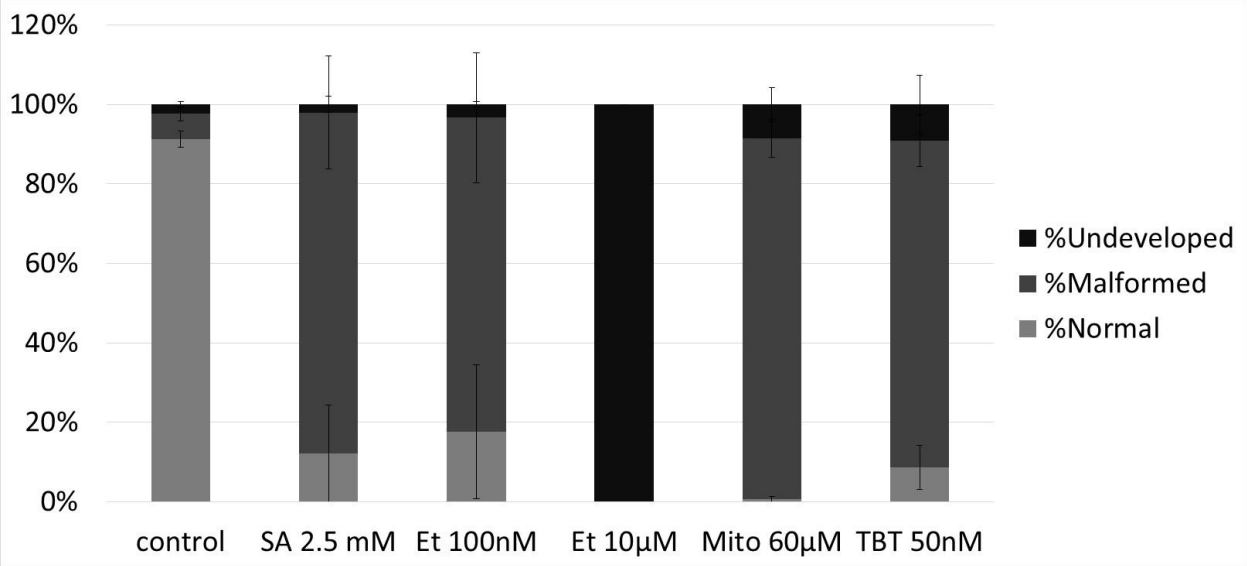

Table 4. Morphometric analysis of phenotypes observed in *Phallusia mammillata* larvae exposed to EDCs. N shows the number of embryos analyzed. The table summarize the following endpoints: ocellus (Oc) + otolith (Ot) area (µm2); Oc/Ot distance (µm); percentage of embryos with palps (%); trunk L/W (length/width) ratio; tail length (µm). All measurements are performed at 22 hpf. Data presented as means ± S.E and as % to the control. Asterisks indicate significant difference compared to the control (Kruskal-Wallis test, $P < 0.05$). BPA indicate bisphenol A ; E2B – estradiol benzoate.

Treatment	N	Oc/Ot area, μm^2, mean ± S.E.	Oc/Ot area % to the control	Oc/Ot distance, µm, mean ± S.E.	Oc/Ot distance % to the control	% palps, means ± S.E.	Palps% to the control	Trunk L/W ratio, means ± S.E.	Trunk L/W % to the control	Tail length, µm, means ± S.E.	Tail length % to the control
control	112	321.1 ± 14.8	-	20.3 ± 1.2	-	80.1 ± 1.6	-	2.2 ± 0.04	-	499.5 ± 12.5	-
Lindane 10µM	136	286.7 ± 12.2	92%	**12.4 ± 1.1** *	**62%**	68 ± 4.5	85%	**1.7 ± 0.02** *	**77%**	489 ± 8	95%
Lindane 15µM	139	**224.4 ± 12.2** *	**71%**	**8.8 ± 1** *	**44%**	60.6 ± 11.1	75%	**1.5 ± 0.02** *	**70%**	476.2 ± 5.4	92%
Lindane 20µM	56	**245.2 ± 16.7** *	**83%**	**8.2 ± 1.3** *	**36%**	52.2 ± 17.2	66%	**1.6 ± 0.04** *	**75%**	443.9 ± 19.4	85%
control	193	293.5 ± 11.2	-	17.1 ± 0.9	-	77.1 ± 7.4	-	1.9 ± 0.03	-	520.1 ± 11	-
Atrazine 25µM	172	262.4 ± 10.8	87%	15.2 ± 1	96%	78.9 ± 8.5	101%	1.8 ± 0.03	94%	525 ± 9.5	101%
Atrazine 50µM	160	274.1 ± 9.8	95%	**14.1 ± 1** *	**83%**	75.1 ± 6.4	102%	**1.7 ± 0.03** *	**92%**	500.4 ± 10.1	99%
Atrazine 70µM	112	277.5 ± 11.7	87%	**13.2 ± 1.2** *	**69%**	85.7 ± 10.7	108%	**1.8 ± 0.03** *	**87%**	554.5 ± 7.2	101%
control	387	294.4 ± 6.8	-	20.4	-	84.1 ± 5.3	-	2.1 ± 0.02	-	535.7 ± 5.9	-
BPA 5µM	165	**124.8 ± 5.7** *	**50%**	**7.6 ± 0.8** *	**38%**	95.9 ± 1.4	98%	2.3 ± 0.03	96%	574.1 ± 6.1	101%
BPA 10µM	343	**91.6 ± 5.3** *	**35%**	**4.4 ± 0.5** *	**26%**	63.7 ± 10	75%	**1.8 ± 0.02** *	**83%**	486.1 ± 6.1	90%
control	195	285.6 ± 10.5	-	17.0	-	78 ± 5.3	-	1.7 ± 0.03	-	521.9 ± 8.3	-
Chlordane 10µM	131	**208.9 ± 11.9** *	**86%**	**11.7 ± 1.1** *	**73%**	52.2 ± 7.9	72%	**1.6 ± 0.03** *	**94%**	476.6 ± 10.6	93%
Chlordane 25µM	101	**199.9 ± 11.9** *	**84%**	**10.5 ± 1.2** *	**64%**	69.9 ± 10.1	95%	**1.6 ± 0.03** *	**96%**	490.7 ± 10.6	93%
Chlordane 50µM	105	**175 ± 11.5** *	**65%**	**6.6 ± 1.1** *	**25%**	65 ± 12.3	85%	**1.5 ± 0.02** *	**92%**	450.6 ± 13.1	86%
control	281	336 ± 6.2	-	21.2 ± 0.6	-	91.1 ± 3.1	-	2.4 ± 0.03	-	562.3 ± 4	-
Chlorpyrifos 10µM	274	**285.6 ± 6.3** *	**85%**	18.1 ± 0.7	76%	77.9 ± 8	85%	**2.2 ± 0.04** *	**89%**	523.8 ± 7.2	90%
Chlorpyrifos 25µM	152	**292.3 ± 6.6** *	**83%**	21.7 ± 0.9	84%	85.9 ± 8.3	90%	2.4 ± 0.04	94%	544.8 ± 8.5	91%
Chlorpyrifos 50µM	216	**245.1 ± 7.2** *	**70%**	**13.8 ± 0.8** *	**52%**	69 ± 13..3	80%	**2.1 ± 0.03** *	**76%**	**464 ± 8.5** *	**66%**
control	193	379.5 ± 9.5	-	24.9 ± 0.7	-	92.8 ± 4.5	-	2.6 ± 0.03	-	461.1 ± 22.5	-
E2B 5µM	159	427.6 ± 4.4	96%	20.7 ± 0.7	85%	98.5 ± 1.5	101%	2.3 ± 0.01	95%	416.1 ± 22.1	94%
E2B 10µM	165	353.8 ± 8.6	95%	20.8 ± 0.9	94%	93.7 ± 5.6	101%	2.4 ± 0.03	96%	482.6 ± 22.8	104%

Figure 3. The percentage of normal (light grey), malformed (dark grey) and undeveloped (black) embryos in the lindane (Lind) 20 µM, atrazine (Atr) 70 µM, bisphenol A (BPA) 10 µM, chlordane (Chl) 50 µM, chlorpyrifos (CP) 50 µM, estradiol benzoate (E2B) 10 µM. Data are presented as means ± SEM.

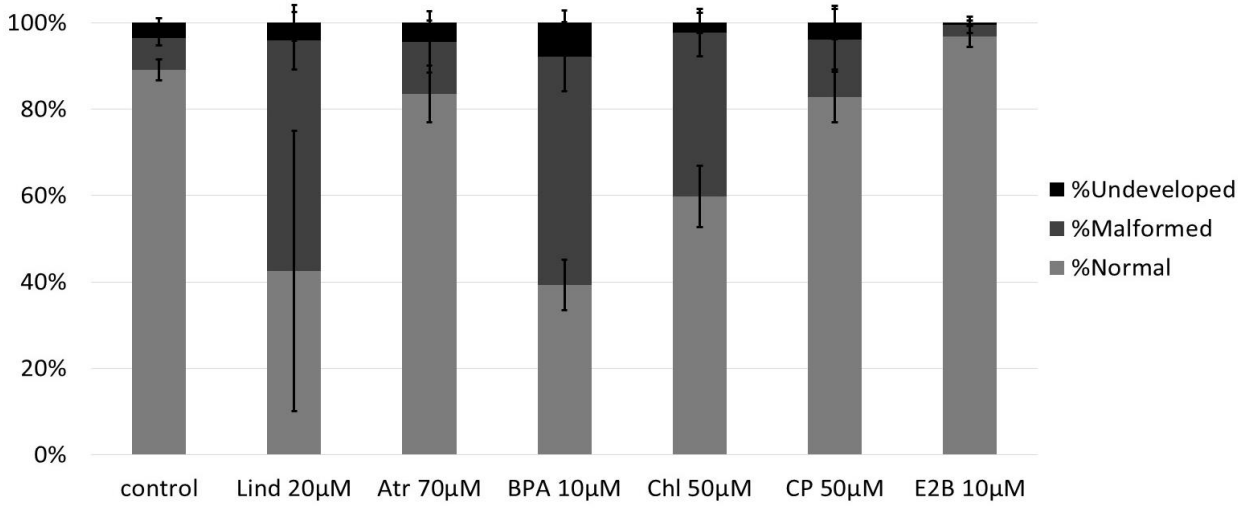

Table 5. Morphometric analysis of phenotypes observed in *Phallusia mammillata* larvae exposed to agonists/antagonists of nuclear receptors (NR). N shows the number of embryos analyzed. The table summarize the following endpoints: ocellus (Oc) + otolith (Ot) area (µm2); Oc/Ot distance (µm); percentage of embryos with palps (%); trunk L/W (length/width) ratio; tail length (µm). All measurements are performed at 22 hpf. Data presented as means ± S.E and as % to the control. Asterisks indicate significant difference compared to the control (Kruskal-Wallis test, $P < 0.05$). ATRA indicate all trans retinoic acid ; 4-OHT – 4-Hydroxytamoxifen ; DES – diethylstilbestrol ; BADGE – Bisphenol A diglycidyl ether.

Treatment	N	Oc/Ot area, μm^2, mean ± S.E.	Oc/Ot area % to the control	Oc/Ot distance, µm, mean ± S.E.	Oc/Ot distance % to the control	% palps, means ± S.E.	Palps % to the control	Trunk L/W ratio, means ± S.E.	Trunk L/W % to the control	Tail length, µm, means ± S.E.	Tail length % to the control
control	468	140.8 ± 3.1	-	14.1 ± 0.4	-	77.1 ± 2.1	-	1.7 ± 0.02	-	416.1 ± 1.7	-
ATRA 0.1µM	385	130.8 ± 4.5	104%	14 ± 0.6	120%	**32.7 ± 6.3** *	**36%**	**1.4 ± 0.01** *	**84%**	404.5 ± 2.4	97%
ATRA 0.5µM	358	**114.7 ± 4.1** *	**103%**	11.7 ± 0.6	122%	**15.9 ± 6.3** *	**23%**	**1.4 ± 0.01** *	**89%**	398.5 ± 2.2	98%
ATRA 1µM	135	162.9 ± 9.9	114%	15.5 ± 1.2	113%	**4.3 ± 2.5** *	**6%**	**1.4 ± 0.02** *	**85%**	410.2 ± 4.9	98%
control	276	137.9 ± 3.6	-	13.8 ± 0.5	-	73.5 ± 3.8	-	1.5 ± 0.02	-	400 ± 2.3	-
BMS493 1µM	241	127.9 ± 4.3	103%	12.3 ± 0.6	101%	54 ± 5	74%	1.6 ± 0.02	99%	395.1 ± 2.6	97%
BMS493 3µM	100	**108.6 ± 5.9** *	**87%**	11.3 ± 1.1	110%	**19.8 ± 7.7** *	**16%**	1.4 ± 0.02	100%	**366.8 ± 8.2** *	**94%**
BMS493 5µM	60	**105.7 ± 6.2** *	**70%**	11.1 ± 1.2	94%	**10.6 ± 6.6** *	**6%**	**1.4 ± 0.02** *	**90%**	**359.9 ± 6.6** *	**87%**
control	139	129.5 ± 4.9	-	13.6 ± 0.7	-	80.4 ± 5.1	-	1.4 ± 0.02	-	356.8 ± 10.7	-
UVI3003 0,1µM	94	130.2 ± 6.1	94%	15 ± 1.1	125%	48 ± 3.2	53%	1.5 ± 0.03	95%	330.2 ± 14.3	96%
UVI3003 1µM	141	**108 ± 4.9** *	**86%**	10.3 ± 0.8	88%	**22.7 ± 8.5** *	**40%**	1.5 ± 0.02	97%	318.2 ± 12.7	100%
UVI3003 2µM	158	**102.3 ± 4.5** *	**75%**	10.3 ± 1.1	82%	**8.3 ± 3.3** *	**23%**	**1.4 ± 0.02** *	**92%**	**237.3 ± 11.5** *	**63%**
control	375	322 ± 6	-	22.9 ± 0.5	-	95.4 ± 3.6	-	2.6 ± 0.03	-	478 ± 14	-
A-OHT 2.5µM	128	**391.1 ± 7.2** *	**103%**	20.6 ± 1.1	96%	95.6 ± 4.4	108%	2.2 ± 0.03	93%	471.5 ± 23.4	100%
4-OHT 5µM	269	290.7 ± 9.7	88%	**12.8 ± 0.9** *	**51%**	**72.8 ± 4.9** *	**79%**	**2.2 ± 0.04** *	**83%**	**416.8 ± 17** *	**88%**
4-OHT 10µM	112	365.7 ± 12.6	100%	**13.5 ± 1.3** *	**60%**	78.4 ± 10.5	87%	**1.9 ± 0.03** *	**77%**	**413.9 ± 25.1** *	**88%**
control	550	326.2 ± 5.4	-	19.7 ± 0.5	-	90.4 ± 4.3	-	2.3 ± 0.02	-	483.7 ± 10.5	-
DES 1µM	464	**285.4 ± 7.1** *	**84%**	**12.9 ± 0.6** *	**64%**	76.9 ± 7.8	85%	**1.9 ± 0.02** *	**80%**	408.4 ± 10	87%
DES 2µM	125	**155.5 ± 11.7** *	**48%**	**8.9 ± 1** *	**44%**	49.7 ± 11.6	52%	**1.6 ± 0.03** *	**69%**	**377.6 ± 17.3** *	**73%**
control	81	280.8 ± 18.9	-	15.1 ± 1.5	-	74.1 ± 5.4	-	1.8 ± 0.07	-	396.7 ± 31.3	-
Rifampicin 50µM	97	308.6 ± 18.9	100%	**9.9 ± 1.2** *	**53%**	55.4 ± 19.9	94%	**1.6 ± 0.05** *	**73%**	328.2 ± 20.6	73%
Rifampicin 100µM	72	236 ± 18.8	94%	**3.1 ± 1** *	**23%**	42.3 ± 18.7	72%	**1.3 ± 0.04** *	**70%**	266.3 ± 27.5	75%
control	306	274.5 ± 7.2	-	21.8 ± 0.7	-	81.1 ± 8.5	-	2.1 ± 0.02	-	434.1 ± 17	-
SR1078 1µM	320	262.5 ± 5.6	99%	19.7 ± 0.7	81%	85.8 ± 5	109%	2.1 ± 0.02	99%	467.4 ± 13.4	104%
SR1078 2µM	223	**255.7 ± 5.4** *	**90%**	22.4 ± 0.7	89%	92.8 ± 2.3	98%	**2.1 ± 0.02** *	**93%**	447 ± 15.8	94%
SR1078 5µM	248	**159.1 ± 7.1** *	**63%**	**7.8 ± 0.7** *	**34%**	51.2 ± 9.9	65%	**1.6 ± 0.02** *	**76%**	**374.8 ± 14** *	**83%**
control	131	322.3 ± 12.7	-	21.3 ± 1.1	-	82.8 ± 5.9	-	2.2 ± 0.03	-	447.5 ± 22.8	-
SR12813 3µM	137	**251.7 ± 10.3** *	**80%**	**13.9 ± 1.1** *	**55%**	77.4 ± 8.9	91%	**2 ± 0.02** *	**84%**	451.4 ± 18.5	101%
SR12813 5µM	225	**185.4 ± 8.2** *	**63%**	**7.5 ± 0.8** *	**32%**	54.1 ± 14.4	63%	**1.7 ± 0.02** *	**72%**	415.7 ± 14.2	93%
SR12813 7.5µM	115	**168.6 ± 12.2** *	**39%**	**13.3 ± 1.3** *	**33%**	**17.8 ± 11.2** *	**41%**	**1.8 ± 0.03** *	**70%**	376.9 ± 24	84%
control	223	340.4 ± 10.2	-	20.4 ± 0.8	-	85.6 ± 9.5	-	2.3 ± 0.03	-	419 ± 28.1	-
BADGE 1µM	113	375 ± 9.2	104%	18.8 ± 1.1	94%	85.2 ± 7.6	104%	**2 ± 0.03** *	**87%**	325.7 ± 26.5	86%
BADGE 2µM	215	338.5 ± 7.6	101%	**13.1 ± 0.8** *	**62%**	84.9 ± 4.8	102%	**1.8 ± 0.02** *	**81%**	378.2 ± 17	102%
BADGE 5µM	198	342.1 ± 6.6	92%	**13.5 ± 0.8** *	**57%**	87 ± 0.8	92%	**1.9 ± 0.02** *	**75%**	354.5 ± 17.6	92%

Table 6. Genotoxicity of toxicants and EDCs in developing embryos of *Phallusia mammillata* (7 – 9 hpf). The number of embryos with DNA aberrations was estimated from images of embryos either at gastrula or early neurula stage, where DNA was stained with Hoechst (Supplementary Fig. 4). The percentage of embryos with DNA aberrations in each culture is shown in the last column.

Tested compound	**Number of embryos with DNA aberrations / total number of embryos imaged**	**The percentage of embryos with DNA aberrations (%)**
0.01% DMSO	0/50	0
Sodium azide 2.5mM	21/30	70
Mitomycin 60µM	32/32	100
Etoposide 100nM	40/59	68
Etoposide 10µM	30/30	100
TBT[1] 50nM	18/25	72
Lindane 20µM	10/20	50
Atrazine 70µM	0/17	0
Chlordane 50µM	5/15	33
Cholrpyrifos 50µM	5/18	27
BPA[2] 10µM	14/119	11

[1]TBT – tributyltin

[2]BPA – bisphenol A

Table 7. Correlation coefficients between % embryos with DNA aberrations, normal, malformed and undeveloped. The t-test is used to establish significance of the correlation between pairs of parameters. Asterisks indicate $p < 0.05$ according to the Spearman's test.

	DNA aberrations (%)	Normal (%)	Malformed (%)	Undeveloped (%)
DNA aberrations (%)	1.00	**-0.93***	0.50	0.35
Normal (%)	**-0.93***	1.00	-0.48	-0.48
Malformed (%)	0.50	-0.48	1.00	-0.12
Undeveloped (%)	0.35	-0.48	-0.12	1.00

Declaration of interests

☒ The authors declare that they have no known competing financial interests or personal relationships that could have appeared to influence the work reported in this paper.

☐The authors declare the following financial interests/personal relationships which may be considered as potential competing interests:

Authors contributions:

Ievgeniia Gazo: performed experiments; participated in data analysis; prepared a draft manuscript. **Isa D. L. Gomes**: performed cultures with BPA; participated in draft preparation. **Thierry Savy**: developed Toxicosis software. **Nadine Peyrieras**: participated in conceptualization of Toxicosis software. **Lydia Besnardeau**: assisted with experiments. **Celine Hebras**: assisted with experiments. **Sameh Benaicha**: data analysis. **Manon Brunet**: performed cultures with ATRA, BMS, UVI. **Olena Shaliutina**: performed cultures with mitomycin. **Alex McDougall**: coordinated the study. **Rémi Dumollard**: coordinated the study, participated in data analysis, edited and rewrote draft